AIP | Applied Physics Letters

Localized surface plasmon resonance of nanoporous gold

Xingyou Lang, Lihua Qian, Pengfei Guan, Jian Zi, and Mingwei Chen

Citation: Applied Physics Letters **98**, 093701 (2011); doi: 10.1063/1.3560482
View online: http://dx.doi.org/10.1063/1.3560482
View Table of Contents: http://scitation.aip.org/content/aip/journal/apl/98/9?ver=pdfcov
Published by the AIP Publishing

Localized surface plasmon resonance of nanoporous gold

Xingyou Lang,[1] Lihua Qian,[1] Pengfei Guan,[1] Jian Zi,[2] and Mingwei Chen[1,a)]
[1]*WPI Advanced Institute for Materials Research, Tohoku University, Sendai 980-8577, Japan*
[2]*Department of Physics, Surface Physics Laboratory, Fudan University, Shanghai 200433, China*

(Received 18 November 2010; accepted 10 February 2011; published online 28 February 2011)

We report the plasmonic properties of free-standing nanoporous gold (NPG) films with an intricate bicontinuous nanostructure. Two characteristic plasmon bands of NPG have been detected in absorption spectra. One at ~490 nm, resulting from the resonant absorption of gold films, is independent of nanopore sizes and dielectric surroundings. The other at ~550–650 nm, arising from the excitation of localized surface plasmon resonance, shows obvious band shift with the nanopore sizes and dielectric indices of surrounding media, suggesting that NPG is a promising candidate as plasmonic sensors for organic and biologic molecule detection. This study also shines light on the underlying mechanisms of surface enhanced spectroscopy of NPG. © *2011 American Institute of Physics*. [doi:10.1063/1.3560482]

Merging photonics and electronics at true nanoscale dimensions, surface plasmonics of nanostructured metals has stimulated considerable interest because of the applications in diverse fields such as optical spectroscopy, photonic devices, and biosensors.[1] Nanoporous gold (NPG) synthesized by chemical/electrochemical dealloying[2,3] has been demonstrated to possess extraordinary optical properties,[4–7] which are ascribed to nanoscale infrastructures of hollow channels and metal skeletons in three dimensions. The interconnected metallic ligaments and hollow channels provide an efficient space for mass transportation of solvents in favor of acquiring a large metal/dielectric interface. Since the unit scale of the metal networks is comparable with the mean free path of conduction electrons in metal ligaments,[8] localized surface plasmon resonance (LSPR) of NPG can be excited within the wavelength range of visible light. The integrated skeleton networks extending to a macroscopic scale also bestow NPG unique properties in plasmonics from the other nanostructures, such as the grating, nanoparticle, and nanorod suspensions.[9–12] For example, NPG membranes exhibit simultaneous excitation of both propagating SPR in planar metal films and LSPR (Ref. 4) and reverse size dependence in surface enhanced Raman scattering and surface enhanced fluorescence.[6,13] It is known that spectral wavelength of LSPR depends on the size and shape of nanostructures and dielectric environments. By detecting peak shift in SPR with refractive indices of dielectric media, metal nanostructures have been exploited as plasmonic sensors.[14–16] Nevertheless, plasmonic properties of NPG have not been comprehensively understood because of their complex three-dimensional (3D) porous structure.[17] In this study we investigate the absorption spectra of NPG with various nanopore sizes in response to the surrounding media and demonstrate that NPG films can be utilized as a promising SPR sensor operated in transmission mode for organic and biologic molecule detection.

NPG films were synthesized by chemically etching $Ag_{65}Au_{35}$ (atomic ratio) leaves with a size of ~20 mm $\times$ 20 mm $\times$ 100 nm in a 70% (mass ratio) HNO_3 solution at room temperature. Nanopore sizes can be tailored from 10 to 50 nm by controlling the corrosion time in the range of 5 min to 24 h. Intermediate porous structure was quenched by distilled water and residual acid within nanopore channels was removed by water rinsing. The fabricated NPG films were placed onto copper grids for microstructural characterization by a JSM 7000F scanning electron microscope (SEM). The nanopore sizes of NPG were determined by statistically measuring the length scales of the nanopores and gold ligaments using a rotational fast Fourier transform method.[17] The concentration of residual silver in the dealloyed NPG films detected by SEM energy dispersive x-ray analysis was smaller than 5 at. %. Ultraviolet-visible (UV-Vis) absorption spectra in the range of 400–850 nm were collected by a JASCO V-650 spectrophotometer with a standard component of ϕ60 mm integrating sphere. During the measurements, the NPG films were sandwiched by two glass slides and solvents were injected into their interstices. The chemical media with variable refractive indices were listed in the following: water (n=1.33), ethanol (n=1.36), 3:1 ethanol/toluene (n=1.39), 1:1 ethanol/toluene (n=1.429), 1:3 ethanol/toluene (n=1.462), and toluene (n=1.495). Scanning rate was 100 nm/min and the bandwidth was selected as 0.1 nm. A baseline correction procedure was executed in the bare glass without a NPG film covering.

Figure 1 shows the representative SEM micrographs of the NPG films with different pore sizes. All specimens exhibit an analogous microstructure in which the hollow channels and gold ligaments look identical in morphology and size. Cross-sectional morphology reveals that nanopores penetrate through the thin films in the lateral direction. The pore sizes can be tuned from 10 to 50 nm by controlling the corrosion time. For example, NPG with a length scale of 10 nm as shown in Fig. 1(a) is formed after 5 min dealloying at room temperature. The significant coarsening of the nanopores and ligaments has been observed with long etching time and, consequently, the pore size of ~50 nm can be achieved after 24 h etching [Fig. 1(b)].

UV-Vis extinction spectra of the NPG films with pore sizes of 10, 15, 20, 25, 30, 40, and 50 nm soaked into the water are shown in Fig. 1(c). Regardless of nanopore sizes, two characteristic resonant bands can be detected in all the NPG samples. The band position at a low wavelength of

a)Author to whom correspondence should be addressed. Electronic mail: mwchen@wpi-aimr.tohoku.ac.jp.

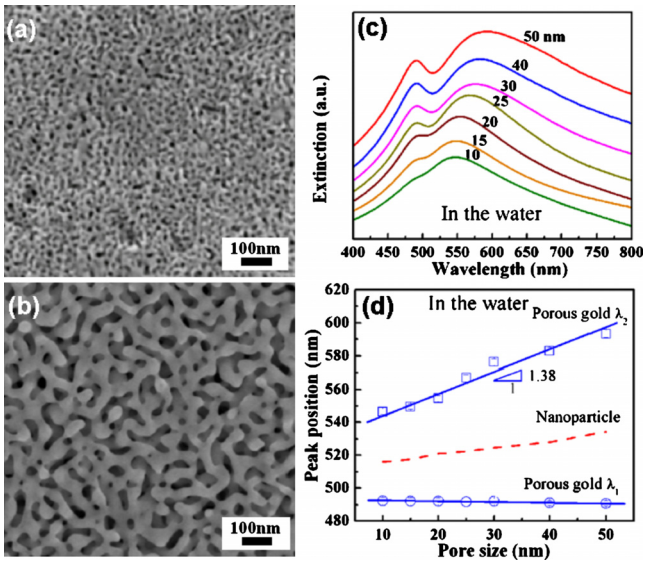

FIG. 1. (Color online) SEM micrographs of NPG synthesized by means of free corrosion for 5 min (a) and 24 h (b). (c) UV-Vis extinction spectra and (d) the resonant peak position of λ_1 and λ_2 of NPG with the pore sizes of 10–50 nm in water. For comparison, the dashed line represents the size dependence resonant band of gold nanoparticles.

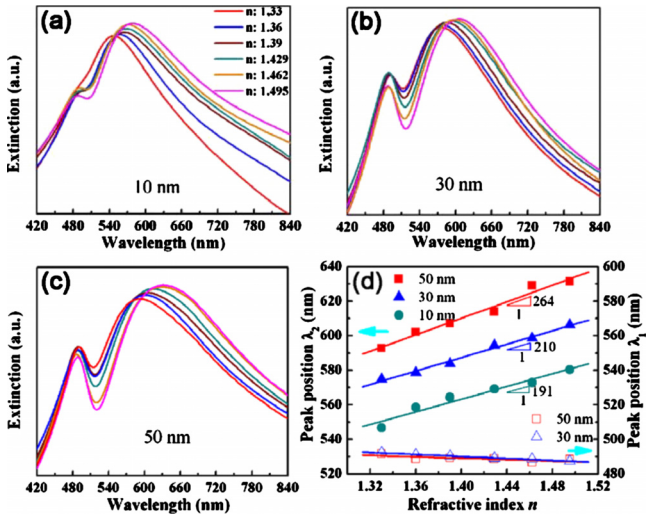

FIG. 2. (Color online) UV-Vis extinction spectra of porous gold films with (a) 10 nm; (b) 30 nm, and (c) 50 nm are recorded by immersing them into various dielectric environments. Refractive index of these solution increases from left to right: water (n=1.33), ethanol (n=1.36), 3:1 ethanol/toluene (n=1.39), 1:1 ethanol/toluene (n=1.429), 1:3 ethanol/toluene (n=1.462), and toluene (n=1.495). (d) Dependence of resonance (λ_1, empty symbols) and LSPR (λ_2, solid symbols) peaks of NPG films on refractive index.

about 490 nm does not change when pore sizes reduce from 50 to 10 nm, whereas the band at a high wavelength shifts from 590 to 545 nm [Fig. 1(d)]. The spectral features of NPG are apparently different from those of other nanostructured gold. For instance, gold nanoparticles are characterized by an isolate SPR band and gold nanorods exhibit one transverse plasmon band at ~520 nm.[18,19] The low wavelength peak of NPG at 490 nm originates from the resonant absorption of gold films.[20] The resonant location mainly relies on film thickness rather than nanopore and ligament sizes. Thus, it is nearly independent of nanopore sizes. In contrast, the high wavelength band, arising from LSPR, represents the significant redshift with the increase in pore sizes, which expectedly results from the effective electron oscillation lengths that are determined by the gold ligament sizes.

Metal nanostructures have been developed as plasmonic sensors based on the SPR band shift with dielectric media.[13–16] Due to the excellent reproduction of absorption spectra and intense SPR peaks, the NPG films can be utilized as reliable plasmonic sensors. Figures 2(a)–2(c) show the extinction spectra of the NPG films immersed into a series of organic dielectric media. The SPR peak at 490 nm (λ_1) does not show detectable shift when the refractive indices of the media (n) increase from 1.33 to 1.495. In contrast, the SPR band at ~540 nm (λ_2) represents evident redshift with the refractive indices. The shift magnitude of λ_2 has a linear relationship with the refractive index as shown in Fig. 2(d), and the sensitivity factor of NPG, defined by the peak shift per refractive index unit (RIU) $d\lambda_2/dn$, can be determined from the slope of the regression line. For the λ_2 SPR band, the NPG films with larger pore sizes show more significant redshift with the refractive index, resulting in larger sensitivity factors of ~210 nm/RIU and ~264 nm/RIU for 30 nm and 50 nm porous gold, respectively [see Fig. 2(d)]. Thus, the refractive index sensitivity of NPG is comparable to those of other nanostructured gold, such as gold nanorods,[19] hollow sphere and cylindrical holes.[21–23] It is known that plasmon coupling occurs when the interspace between neighboring nanostructured metals is smaller than 10–20 nm, which leads to the reduction in plasmonic sensitivity. Apparently, the nanopore size dependence of the sensitivity factors of NPG, i.e., sensitivity factors decrease with nanopore sizes, is associated with the increased plasmon coupling between gold ligaments in NPG with a nanopore size smaller than 20 nm.

Because of the recognizable dependence of plasmonic sensitivity on the nanopore sizes, the NPG films with different pore sizes give rise to distinct plasmon peak shift even in the same surrounding media [Figs. 1(c) and 1(d)]. This can be employed for the application in biosensors for molecule identification by measuring the dependence of the plasmon peak shift with nanopore sizes. Figure 3(a) shows an example of the detection of human serum albumin (HSA), in which the λ_2 peak of the UV/Vis spectra of HSA coated NPG significantly redshift with the increase in nanopore sizes. In contrast, only very limited peak shift can be observed in the extinction spectra of bare NPG films in air and water. Figure 3(b) illustrates the linear relationship of plasmon peak positions of NPG films as a function of pore size with the slopes of $\Delta\lambda/\Delta d \approx 1$, 1.4, and 2.8 for the surrounding media of air, water, and HSA, respectively. From the obvious difference in the slopes, we can easily determine the molecules with different dielectric constants. Since the overlapping between

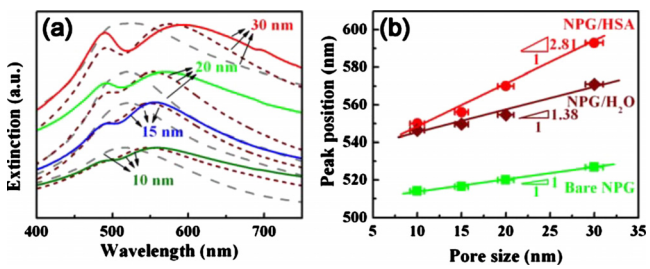

FIG. 3. (Color online) (a) UV-Vis extinction spectra and (b) pore size dependence of plasmon peak of bare NPG in air (dashed lines), in water (short dashed lines) and NPG coated with HSA monolayer (solid lines).

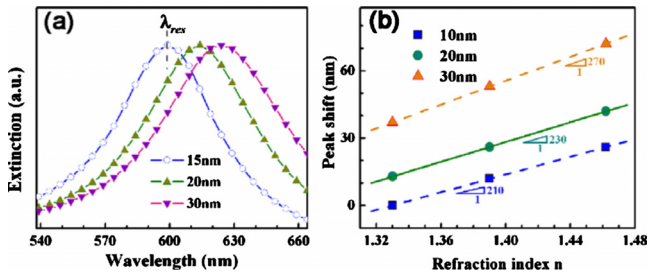

FIG. 4. (Color online) (a) DDA simulated SPR spectra of NPG with various nanopore sizes. (b) The relationship between the SPR band of NPG and dielectric index of a surrounding medium.

low and high wavelength bands, the patterns of NPG in air only show one broad band, which looks different from those of the NPG films in other surroundings with large dielectric indices, i.e., the UV-Vis spectra clearly show both low and high wavelength plasmon bands as a result of the redshift in the surface plasmon band (λ_2) while the low wavelength plasmon band (λ_1) remains constant. In view of the obvious changes in the slopes, $\Delta\lambda/\Delta d$, with the different dielectric surrounding media, the UV-Vis extinction spectra of the NPG with different pore sizes can thus be utilized to detect adsorbed organic and biomolecules by measuring the nanopore size dependence of the plasmon band (λ_2) shift.

The surface plasmonic properties of NPG were further investigated by near-field electromagnetic calculations using a discrete dipole approximation.[24] A quasi-3D model abstracted from the real structure of NPG measured by electron tomography[17] has been developed to describe a simplified local configuration of NPG with the variation in characteristic porous size and ligament length.[25] The extinction spectra of this system have been calculated by considering external light incident normal to the top surface of the nanostructure. The peak positions of these spectra are corresponding to the SPR wavelength λ_2. Due to the nonperiodicity of the nanostructure in the simulation, we cannot obtain the SPR band λ_1 at ~490 nm that comes from the resonance of the gold films. Figure 4(a) shows the SPR spectra of simulated NPG with different nanopore sizes (D), in which λ_2 shifts to red accompanying with the decrease in the intensity of localized electromagnetic fields when the nanopore sizes increase. The trend of peak shift with the characteristic nanopore size is well consistent with the experimental observations (Fig. 2). In order to understand the dependence of λ_2 on dielectric environments, the extinction spectra are calculated by using a relative refractive index of a medium. The shift magnitude of λ_2 linearly depends on the refractive index as indicated in Fig. 4(b), agreeing with the experiment that the LSPR band, λ_2, is sensitive to dielectric environments. The refractive index sensitivity of NPG depends on the nanopore sizes and increases from 200 to 270 nm/RIU with the nanopore sizes from 10 to 30 nm, again well consistent with the experimental observations (Fig. 4).

In summary, NPG films with 3D bicontinuous nanoporosity possess unique optical response with two characteristic SPR bands in absorption spectra. The resonant peak from LSPR excitation represents remarkable redshift with pore sizes and dielectric media, demonstrating that the NPG films can be utilized as plasmonic sensors. Moreover, the biocompatible NPG with a uniform nanostructure can be fabricated in the form of free-standing films for direct use in SPR devices without the requirement of a complex assembly process.

[1]E. Ozbay, Science **311**, 189 (2006).
[2]A. J. Forty, Nature (London) **282**, 597 (1979).
[3]J. Erlebacher, M. J. Aziz, A. Karma, N. Dimitrov, and K. Sieradzki, Nature (London) **410**, 450 (2001).
[4]F. Yu, S. Ahl, A. M. Caminade, J. P. Majoral, W. Knoll, and J. Erlebacher, Anal. Chem. **78**, 7346 (2006).
[5]J. Biener, G. Nyce, A. M. Hodge, M. M. Biener, A. V. Hamza, and S. A. Maier, Adv. Mater. **20**, 1211 (2008).
[6]L. H. Qian, X. Q. Yan, T. Fujita, A. Inoue, and M. W. Chen, Appl. Phys. Lett. **90**, 153120 (2007).
[7]M. C. Dixon, T. A. Daniel, M. Hieda, D. M. Smilgies, M. H. W. Chan, and D. L. Allara, Langmuir **23**, 2414 (2007).
[8]T. Fujita, H. Okada, K. Koyama, K. Watanabe, S. Maekawa, and M. W. Chen, Phys. Rev. Lett. **101**, 166601 (2008).
[9]M. E. Stewart, C. R. Anderton, L. B. Thompson, J. Maria, S. K. Gray, J. A. Rogers, and R. G. Nuzzo, Chem. Rev. **108**, 494 (2008).
[10]K. Raether, *Surface Plasmons on Smooth and Rough Surfaces and Gratings* (Springer, Berlin, 1988).
[11]C. F. Bohren and D. R. Huffman, *Absorption and Scattering of Light by Small Particles* (Wiley, New York, 1998).
[12]S. Link, M. B. Mohamed, and M. A. El-sayed, J. Phys. Chem. B **103**, 3073 (1999).
[13]X. Y. Lang, L. Zhang, P. F. Guan, T. Fujita, and M. W. Chen, Appl. Phys. Lett. **96**, 073701 (2010).
[14]M. D. Malinsky, K. L. Kelly, G. C. Schatz, and R. P. Van Duyne, J. Am. Chem. Soc. **123**, 1471 (2001).
[15]X. Xu and M. B. Cortie, Adv. Funct. Mater. **16**, 2170 (2006).
[16]J. Homola, *Surface Plasmon Resonance Based Sensors* (Springer, Berlin, 2006).
[17]T. Fujita, L. H. Qian, K. Inoke, J. Erlebacher, and M. W. Chen, Appl. Phys. Lett. **92**, 251902 (2008).
[18]T. Okamoto, I. Yamaguchi, and T. Kobayashi, Opt. Lett. **25**, 372 (2000).
[19]S. M. Marinakos, S. H. Chen, and A. Chilkoti, Anal. Chem. **79**, 5278 (2007).
[20]U. Kreibig and M. Vollmer, *Optical Properties of Metal Clusters* (Springer, Berlin, 1995).
[21]A. Dahlin, M. Zäch, T. Rindzevicius, M. Käll, D. S. Sutherland, and F. Höök, J. Am. Chem. Soc. **127**, 5043 (2005).
[22]D. Gao, W. Chen, A. Mulchandani, and J. S. Schultz, Appl. Phys. Lett. **90**, 073901 (2007).
[23]A. Lesuffleur, H. Im, N. C. Lindquist, and S. H. Oh, Appl. Phys. Lett. **90**, 243110 (2007).
[24]B. T. Braine and P. J. Flatau, User guide for the discrete dipole approximation code DDSCAT7.0, http://arxiv.org/abs/0809.0337
[25]X. Y. Lang, P. F. Guan, L. Zhang, T. Fujita, and M. W. Chen, J. Phys. Chem. C **113**, 10956 (2009).